Tailor-Made Polymers for Laser Ablation

Thomas LIPPERT, Christian DAVID, Marc HAUER, Claude PHIPPS,* and Alexander WOKAUN

Paul Scherrer Institut, 5232 Villigen PSI, Switzerland

**Photonic Associates, 200A Ojo de la Vaca Road, Santa Fe 87504, USA*

(Received June 18, 2001)

Photopolymers based on triazene-groups were designed for UV laser ablation. The tested triazene-polymer reveals a low threshold fluence and unusually high ablation rates at low and high fluences. The polymer decomposes into gaseous products, resulting in clean ablation structures without surface contaminations. The triazene-polymer was also tested for two different applications at two different irradiation wavelengths, i.e. in the UV (308 nm) and in the near-IR (935 nm). Diffractive gray tone phase masks optimized for laser ablation were applied to fabricate microoptical elements. The triazene-polymer reveals also superior properties for applications in the near-IR. Near-IR irradiation is used to create a plasma which could be used as thruster for microsatellites. The carbon-doped triazene-polymer shows higher values of the momentum coupling coefficient and specific impulse than a commercial polymer. The well-defined threshold for the maximum momentum coupling coefficient was only observed for the designed polymer.

Key Words: Photopolymer, Ablation, Microoptics, Phase mask, Laser plasma thruster

1. Introduction

Laser ablation of polymers was first reported in 1982[1,2] and envisioned as a possible alternative or complementary technique to conventional photolithography, but has unfortunately several disadvantages, i.e. carbonization upon irradiation,[3] and debris contaminating the surface and optics. Other major concerns for industrial applications, especially of UV-lasers, are the high cost of photons and the efficient utilization of the photons, i.e. the sensitivity of the polymers to laser irradiation.[4] To overcome these limitations, novel photopolymers were developed for ablation at a specific irradiation wavelength, i.e. 308 nm.[5-9] Photochemical considerations have been applied for the design of these polymers. The irradiation wavelength of 308 nm was chosen because of the convenience of this wavelength from a practical point of view, i.e. lifetime of the optical components and gas fills of the XeCl excimer laser, and because sub-micron resolution is not necessary for all applications. For an irradiation wavelength of 308 nm, it is possible to selectively excite the absorption band of the photochemically active chromophore. This can give indications about the role of the photochemically active chromophore during the ablation process and therefore the ablation mechanism. It is still not clear whether the ablation mechanism is purely photothermal or has at least partly photochemical features. The latter has been suggested for shorter irradiation wavelengths, e.g. 193 nm.[10] The most promising approach for the design of these 'laser ablation polymers' is the incorporation of the photochemically active chromophore into the polymer main chain. These polymers are highly absorbing at the irradiation wavelength and decompose exothermally at well-defined positions of the polymer chain into gaseous products.[11] The gaseous products act as driving gas of ablation and carry away larger fragments, which could otherwise contaminate the surface. The polymers are ablated without major modifications of the residual polymer surface,[12] thus allowing reproducible ablation.

Complex patterns, e.g. microoptical elements, can either be generated by scanning ablation tools, which are even capable of producing continuous topographies by varying the applied fluence on the material surface.[13] Due to the sequential nature of the method, the throughput is very limited. A parallel patterning of larger areas requires a set-up comparable to photo steppers, where the mask structure is projected onto the substrate surface.[14] One of the major problems of this method is the damage occurring in chromium absorber structures of standard photomasks at higher laser fluences.[15] An alternative technique utilizes diffractive grating structures etched into a quartz mask blank to diffract the transmitted light out of the aperture of the projection optics.[16] This method combines the capability of scanning ablation tools to vary the ablated depth continuously with the high throughput of projection methods. An additional improvement can be achieved by the application of special photopolymers. The possible resolution of ≤ 1 μm with our set-up is also sufficient for many applications.

A very different application of laser ablation of polymers can be found in aerospace science. With the advent of microsatellites (> 10 kg), nanosatellites (1-10 kg) and even picosatellites (< 1 kg) it is necessary to develop steering engines which have a small mass (≤ 200 g) and size, produce a high specific impulse and are inexpensive. One promising candidate for this application are laser plasma thrusters (LPT's),[17,18] which have some advantages over more common candidates for microthrusters, such as pulsed plasma thrusters or resistojets. One quite serious problem with existing nozzle thrusters is that unpredictable physical regimes are entered when the dimension of the nozzles are so small that the gas flow can no longer be described by the theory of viscous flow, what is the case for a 1 μm nozzle at pressure of 10 bar. Nozzles are not necessary for LPT's, because the plasma expan-

sion is already similar to a nozzle expansion. One other advantage of a LPT is the possible higher maximum specific impulse (see below) and the high efficiency of ≈ 50 %. For chemical rockets the maximum impulse is about 500 s, limited by the available temperatures, while a specific impulse of 8000 s was reported for laser ablation of Al.[19] Due to the specific demands, i.e. weight and power, of small satellites, small powerful (≥ 1 W) diode laser must be used. These lasers emit in the near-IR (930-980 nm), with an available power of around 1-5 Watt and pulse lengths from 100 µs to the ms range. Fluences of several hundred J cm^{-2} can be achieved with standard optical components (laser spot diameter around 5 µm). The long pulse lengths of the diode lasers restrict the applicable materials to polymers, which have low thermal conductlvities. It was for example not possible to create a plasma with the previously mentioned diode lasers on Al. The performance of the LPT's is to a large extent depending on the properties of the polymers used in these devices.

The clean ablation structures, low ablation rate and well-defined exotherntic decomposition of the triazene-polymer was an attractive feature to test this polymer also for microstructuring and for application in LPT's.

2. Experimental

The synthesis of the triazene-polymer (TP, structure shown in Fig.1, left) was described in detail elsewhere.[20] A XeCl excimer laser (Lambda Physik Compex 205; λ = 308 nm, τ = 20 ns) was used as irradiation source. The polymer films (50 µm thick) for the laser ablation experiments were prepared by solvent casting with THF or chlorobenzene as solvent. The procedure for determining the etch rates has been described in detail elsewhere.[21] The ablation experiments were performed at low (10-400 mJ cm^{-2}) and high fluences (up to 20 J cm^{-2}) to investigate the ablation behavior.

Thin films (1-5 µm thick) of the triazene-polymer were spincoated onto quartz wafers for the fabrication of microoptical elements. As spincoating solution 15 wt.% of the polymer in chlorobenzene were used. The polyimide (125 µm thick sheets of Kapton® from Goodfellow) was used as received. The phase masks were prepared by electron beam lithography, as reported elsewhere.[22]

For the carbon-doped triazene-polymer films, chlorobenzene was used as solvent, while for the carbon-doped polyvinylalcohol (PVAlc, Alcotex™, Hoechst; Fig.1, right) a water/methanol mixture was used. The amount of carbon was adjusted to obtain optical densities between 1 and 2.5. Various carbon materials were tested, i.e. Ketjen Black (conducting carbon), Printex A (basic carbon) from BASF and black pearls (diameter 15 nm) from Cabot. The polymer solutions were combined with carbon suspensions (prepared with a high speed stirrer, Ultra-Turrax T25, in the same solvent as the polymer) and mixed with the high-speed stirrer. The films (≥ 60 µm) were prepared by drawing (draw blade applicator, Industry Tech) the suspensions onto polymer substrates (PET and Kapton). The performance

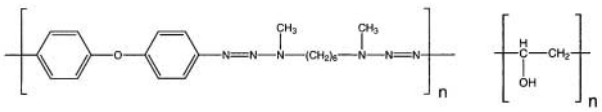

Fig.1 Chemical structures of the polymers; triazene-polymer (left) and poly-vinylalcohol (right).

of the films was determined by irradiation with a diode laser (SDL, Inc. XC30) and a special developed torsion balance (sensitivity as low as 10^{-10} N s), described in detail elsewhere.[18]

3. Results and Discussion

3.1 Ablation characteristics

The ablation characteristics of the triazene-polymer (TP) were studied over a broad fluence range, i.e. from 10 mJ cm^{-2} to 20 J cm^{-2}. The etch rates (etch depth/pulse) were calculated from linear plots of the etch depths vs. pulse number at a given fluence. All plots were linear, showing no incubation behavior as expected for highly absorbing polymers with a linear absorption coefficient, α_{lin}, of ≈ 100,000 cm^{-1} at the irradiation wavelength of 308 nm.

The high fluence range is mainly interesting for applications where high ablation rates in small areas are important, e.g. drilling or cutting. The low fluence range offers the opportunity to study the influence of structural parameters on the ablation rates. The low fluence range is also important for lithographic applications, where the cost of the photons is important. Low fluences are defined in this study from 10 to 500 mJ cm^{-2} . A plot of the etch rates versus fluences not the (normally applied logarithmic fluence scale) is shown in Fig.2.

The effective absorption coefficient, α_{eff}, and threshold fluences, F_{th}, were F_{th} were calculated at low fluence according to Equation (1),[23,24]

$$d(F) = \frac{1}{\alpha_{eff}} \ln\left(\frac{F}{F_{th}}\right) \qquad (1)$$

where d (F) is the etch rate (etch depth per pulse). The threshold fluence of 25 mJ cm^{-2} agrees very well with previously obtained values.[25,26] The effective absorption coefficient is about half (α_{eff} ≈ 50000 cm^{-1}) of the linear (Lambert Beer) absorption coefficient, including bleaching of the triazene chromophore during the excimer pulse.[25] This bleaching is most probably the decomposition of the triazene group during the laser pulse, as suggested by ns-interferometry, where etching of the polymer was observed within the laser pulse.[27] The etch rates at low fluences, e.g. of ≈ 265 nm at 100 mJ cm^{-2}, are to our knowledge, the highest reported values for a polymer. The TP shows also a remarkably high etch rate of more than 3 µm per pulse at the highest applied fluences, which is aiso among the highest for synthetic pure polymers. The etch rate for a commercial polymer with a similar α_{lin}, e.g. polyimjde, is only half of this value.[28] The ablation structures are very well-defined with no visible heat

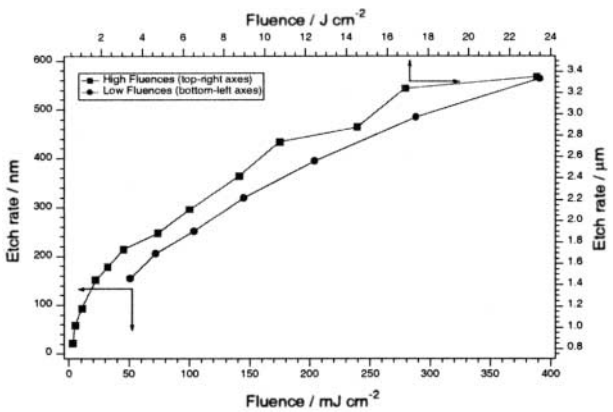

Fig.2 Measured etch rates as a function of the fluence. Irradiation wavelength 308 nm.

affected zone or debris contaminating the surrounding of the structure (shown in Fig.3). In the case of polyimide carbon-debris is detected in and around the ablation structure.[3] The structure is created by imaging a slit mask onto the sample surface, using an Schwarzschild type reflecting objective with a demagnification of 15:1.

3.2 Laser ablation applied for the fabrication of microoptical elements

The above described ablation properties encouraged us to develop special phase mask for laser ablation. The phase mask were designed for 308 nm as irradiation wavelength using an 80 mm focal length projection lens at demagnification factors between 2 and 4. The grating pitch was kept constant at 3 μm, which provides a sufficiently high deflection angle of the diffracted light. Only the 0^{th} order was used for the structuring (higher orders were blocked by an aperture) as shown in Fig.4. The zero order efficiency of the phase mask can be calculated by simple scalar diffraction theory and depends on the duty cycle. The duty cycle is defined as the ratio between the spacing of the grating line widths and the grating period. At a duty cycle of 0.5 the zero order diffraction efficiency is 0, when the depth of the grating structures is matched to give a phase shift of π. The ablation depths were measured after ablation using phase masks with various duty cycles. The ablation depths follow the theory quite well. The deviations can be explained by the non-linear ablation behavior (see Fig.2) and the existence of a fluence threshold for ablation. Including these parameters into the design of the phase masks improves the efficiency of the ablated structures, e.g. gratings, by a factor of 2.[16] An example of the improved quality of blazed gratings in polyimide fabricated by laser ablation is shown in Fig.5. The profilometer traces of the uncorrected structure resemble more an interference grating than a blazed grating. After correction for the threshold and non-linear etch rate, profiles are obtained which resemble blazed gratings quite well.

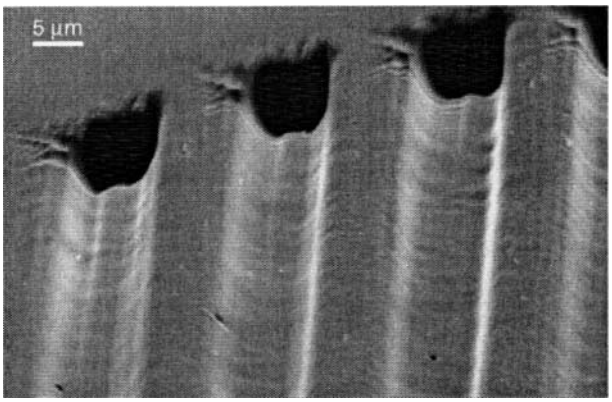

Fig.3 SEM micrograph of a microstructure in the triazene-polymer: 5 pulses with ≈ 5 J cm^{-2} at 308 nm.

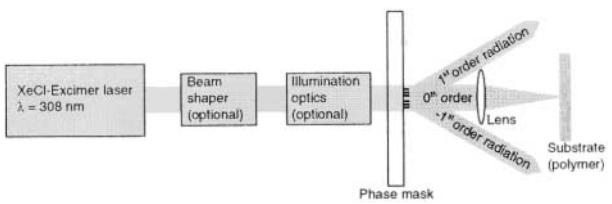

Fig.4 Scheme of the set-up for the patterning of polymer surfaces by laser ablation using diffractive masks.

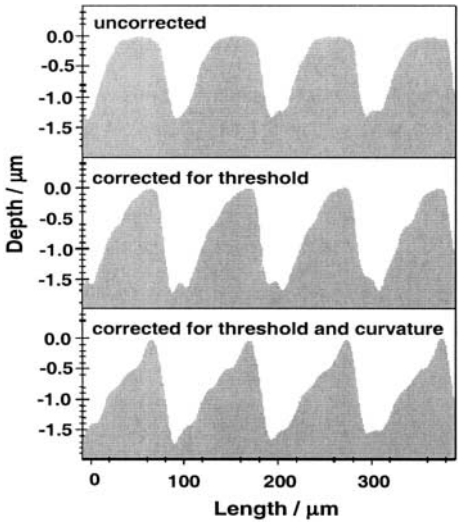

Fig.5 Profilometer scans of blazed grating structures in PI using the set-up in Fig.4. The profile shape depends on the corrections for the polymer response curve, i,e. existence of threshold fluence and non linear ablation rate, into the mask design.

Further improvements should be possible by a more sophisticated correction for the phase masks and the application of our designed photopolymers.

Various structures were ablated into TP and polyimide (PI). Polyimide was again selected as reference polymer, because the absorption coefficient (100000 cm^{-1}) is comparable to TP, but with a higher threshold (60 mJ cm^{-2}) and lower etch rates (e.g. of 61 nm $pulse^{-1}$ with 100 mJ cm^{-2}). For polyimide a photothermal ablation mechanism is generally accepted at longer wavelengths,[10] while it has been suggested that that the triazene-polymer ablation is mainly photochemical.[6] It has been shown, that the decomposition products of the triazene polymer are malnly gaseous[11] which do not contanunate the surface, without modification of the remaining polymer surface.[12] In the case of polyimide and most commercial polymers, solid ablation products (debris) and carbonization of the polymer surface has been detected.[3] An example of Siemens stars etched into TP (left) and PI (center) is shown in Fig.6. The modified and re-deposited material is clearly visible around the ablated structure of the PI (center), but is absent for TP (left). A 4 × magnification of Siemens star in the center is shown in Fig.6 (right). It is clearly visible that the deposited material originates from ablation structures. A closer microscopic examination and studies using Raman-microscopy[3] and imaging x-ray photoelectron spectroscopy[28] have shown that carbonization takes also place inside the ablated structures. Any surface contamination or modification will deteriorate the performance of the microoptical ele-

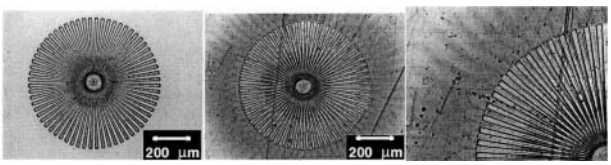

Fig.6 Micrographs of Siemens stars fabricated by laser ablation. Triazene-polymer (left) and polyimide (center) and 4 × magnification of the center micrograph (right). 5 pulses at 308 nm.

ments and render the ablation rates unpredictable. An example of a Fresnel lenses etched into the triazene-polymer is shown in Fig.7. The ablation structures are well defined (shown in Fig.7, left), and even arrays of structures (Fig.7, right) can be created fast and easy. The higher sensitivity and etch rates of the triazene-polymer allows the application of larger phase masks. Alternatively, less pulses are necessary to fabricate an optical element with a given depths of the structures.

The combination of gray tone phase masks with the highly sensitive photopolymers is suitable for the fast fabrication of 3-dimensional topographies. Single laser pulses can create complex structures, such as Fresnel lenses. A pattern transfer into glass or quartz, e.g. by proportional etching techniques, would open an even larger spectrum of applications.

3.3 Polymers for laserplasma thrusters (LPT)

One property of the triazene-polymer is the exothermic decomposition and the 'weak' =N - N< bond in the polymer. This weak bond is probably also the primary decomposition site for near-IR irradiation wavelengths, which will result in thennal decomposition.

In order to measure impulses 5 orders of magnitude upwards from nano N-s, one of the most sensitive torsion pendula was constructed.[18] The pendulum was statically calibrated (force calibration) and then used to analyze the performance of the polymer films for LPT's. The target momentum was measured by the torsion balance and used to calculate the momentum coupling coefficient, C_m. This quantity is defined as

$$C_m = \frac{m\Delta v}{W}$$

with $m\Delta v$ as the target momentum produced during the ejection of laser-ablated material. W is the incident laser pulse energy. Another important parameter for thrusters is the specific impulse I_{sp}, which is defined as

$$C_m Q^* = v_E = I_{sp} g$$

Q^* is the specific ablation energy (incident power/mass ablation rate), v_E is the exhaust velocity and g is the acceleration due to gravity. In other words, I_{sp} is the time for which an acceleration of g would have to act to bring the exhaust mass up to the velocity v_E. A scheme of an envisioned design for the LPT's is shown in Fig.8. Two geometries are possible, i.e. reflection mode, which has the advantage of 2 times higher I_{sp} and C_m, but the disadvantage of an awkward geometry which requires additional shielding for the optical components. The transmission mode has the better geometry and the protected optics, but the disadvantage of a 2 times lower I_{sp} and C_m.

The following measurements were performed in the transmission mode. Two polymers were selected for the tests, i.e. TP

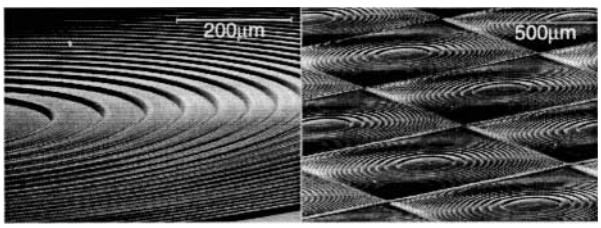

Fig.7 SEM images of diffractive lenses fabricated by laser ablation. Magnification of one lens (left) and array of lenses (right).

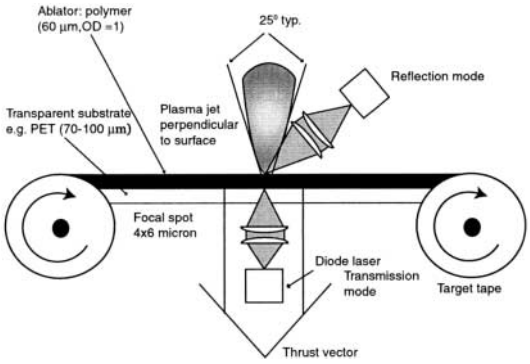

Fig.8 Scheme of the possible design for LPT's.

and a commercial polymer (poly-vinylalcohol, PVAlc). Both polymers pass the fundamental requirements for LPT's. The polymers give homogenous films with a good adhesion on PET; they do not stick to each other; they are elastic over a broad temperature range (- 50 to + 60 ˚C) and have an optical density (OD) of about 1-2.5. The latter requires that it is possible to dope the films homogenously with carbon. Most polymers have to be doped to accomplish an effective absorption in the near-IR. Carbon was chosen as dopant due to the broad homogenous absorption over the whole near-IR range. The films of both polymers were prepared with an optical density between I and 2.5 and a thickness between 20 and 70 µm. The 70 µm are the upper limit which can be accomplished for these polymers by our preparation method and tools.

In Fig.9, the momentum coupling coefficients and specific impulse at various laser fluences of the carbon-doped triazene polymer and of a carbon-doped PVAlc are shown. The triazene-polymer reveals higher coupling coefficients and, more importantly, a quite well defined threshold for a maximum C_m The carbon-doped triazene polymer clearly reveals a higher specific impulse than the poly-vinylalcohol. The fewer data points for the triazene polymer are due to the very irregular shape of the craters which did not allow measurements of the ablated volume at all laser fluences. The I_{sp} values are clearly higher for the triazene-polymer, and probably reveal a maximum at a similar fluence range as for C_m.

As substrates PET (clear Mylar with 91 % transmission at 935 nm for 100 µm, and opaque Mylar with 69 % transmission at 935 nm for 75 µm) and Kapton (79 % transmission at 935 nm for 75 µm) were tested. As expected, better performance (C_m)

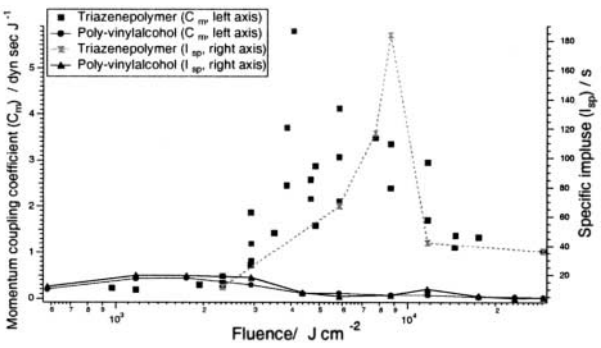

Fig.9 Momentum coupling coefficient (impulse/1aser energy) and specific impulse at various fluences for the carbon-doped polymers (triazene-polymer and poly-vinylalcohol). Optical density at 935 nm ≈ 0.9, film thickness ≈ 65 µm, PET substrates.

was obtained for the substrates with higher transmission. The thickness of the substrates has a pronounced influence on the measurements. For substrates thinner than 75 μm a negative momentum was observed. This was caused by the burnthrough of the substrates, which was not observed for uncoated substrates, even at much higher fluences. Therefore it c an be assumed that the carbon-doped polymers start to decompose at the interface to the substrate, causing also the decomposition of the PET or Kapton. When the substrate burns through faster than the coated polymer a negative momentum is detected. This was confirmed by holes in the substrates after these experiments. The influence of other tested parameter on C_m can only be described qualitatively until sufficient data are accumulated. The general trends are: Higher optical densities (within the tested range of 1 to 2.5) and larger thickness (up to 70 μm) are better. The different carbon dopants can be ranked from black pearls > conducting carbon ≥ basic carbon.

The well-defined threshold and higher C_m of the triazene-polymer is an important feature for the design of a plasma thruster with tape-like polymer fuel, because the optimum incident laser fluence and tape speed are clearly defined. The decreasing values of C_m after the maximum are due the increasing fraction of incident laser energy devoted to accelerating vapor, then creating plasma and to absorption of the laser energy by the crated plasma.[29] The well-defined threshold and higher values are probably due to the decomposition properties of the triazene-polymer. The thermal decomposition, initiated by absorption of the laser energy by the carbon, follows most probably the same pathway as the UV Iaser-induced decomposition. The N_3-group is the photolabile group in the polymer, but also the primary decomposition site of thermolysis, as suggested by product analysis by mass spectrometry.[30]

If the thermally induced decomposition follows the same pathway as the UV laser induced decomposition, then it could be possible to select the polymers for LPT's according to sirDilar principles as for UV laser ablation. The most important design features for polymers designed for UV laser ablation are: an exothermic decomposition into gaseous products; well-defined primary decomposition sites in the polymer main chain; and a high absorptivity at the irradiation wavelengths.

4. Conclusion

Photopolymers based on triazene-groups were designed for uv laser ablation at 308 nm. The selected polymer reveals low threshold fluences and high ablation rates at low and high fluences. The polymer decomposes into gaseous products, resulting in clean ablation structures without surface contaminations. The combination of phase masks and triazene-polymers can be used to fabricate fast 3-dimensional topographies using laser ablation. The enhancements of the phase mask design, by incorporating the ablation behavior of the polymer into the mask design, and the application of photopolymers, which decompose without contamination of the surface, improved the quality of the microoptical elements.

The triazene-polymer reveals also superior properties for applications in laser plasma thrusters using near-IR irradiation. The carbon-doped triazene-polymer shows higher values of C_m and I_{sp} as compared to a commercial polymer (PVAlc). The well-defined threshold for the momentum coupling coefficient is an important aspect for the application of polymers in laser plasma thrusters.

Acknowledgements

This work has been supported by the Swiss National Science Foundation, a NATO Grant for international collaboration (CRG 973063), and by the U.S. Air Force Office of Scientific Research (STTR Phase 11 contract No. F49620-98-C-0038). BASF and BAYER have made some materials available.

References

1) R. Srinivasan and V. Mayne-Banton: Appl. Phys. Lett. **41** (1982) 576.
2) Y. Kawamura, K. Toyoda, and S. Namba: Appl. Phys. Lett **40** (1982) 374.
3) F. Raimondi, S. Abolhassani, R. Brutsch, F. Geiger, T. Lippert, J. Wambach, J. Wei and A. Wokaun: J. Appl. Phys. **88** (2000) 1.
4) K. Suzuki, M. Matsuda, T. Ogino, N. Hayashi, T. Terabayashi, and K. Amemiya: *Proc. SPIE* **2992** (1997) 98.
5) T. Lippert, J. Stebani, J. Ihlemann, O. Nuyken, and A. Wokaun: Angew. Makromol. Chem. **206** (1993) 97.
6) T. Lippert, J. Stebani, J. Ihlemann, O. Nuyken, and A. Wokaun: J. Phys. Chem. **97** (1993) 12296.
7) T. Lippert, T. Kunz, C. Hahn, and A. Wokaun: Recent Res. Devel. in Macromol. Res. **2** (1997) 121.
8) O. Nuyken, U. Dahn, N. Hoogen, D. Marquis, M. N. Nobis. C. Scherer, J. Stebani, A. Wokaun, C. Hahn, Th. Kunz, and T. Lippert: Polym. News **24** (1999) 257.
9) O. Nuyken, C. Scherer, A. Baindl, A. R. Brenner, U. Dahn, R. Gärtner, S. Kaiser-Röhrich, R. Kollefrath, P. Matusche, and B. Voit: Prog. Polym. Sci. **22** (1997) 93.
10) S. Kuper, J. Brannon, and K. Brannon: Appl. Phys. A **56** (1993) 43.
11) L. S. Bennett, T. Lippert, H. Furutani, H. Fukumura, and H. Masuhara: Appl. Phys. A **63** (1996) 327.
12) T. Lippert, T. Nakamura, H, Niino, and A. Yabe: Macromolecules **29** (1996) 6301.
13) N. H. Rizvi, P. T. Rumsby, and M. C. Gower: *Proc. SPIE* **3898** (1999) 240.
14) E. C. Harvey and P. T. Rumsby: *Proc. SPIE* **46** (1998) 26.
15) J. T. Yeh: *Proc. SPIE* **922** (1988) 461.
16) C. David, J. Wei, T. Lippert, and A. Wokaun: Microlectr. Engineering (2001) in press.
17) C. R. Phipps and J. Luke: *Proc. SPIE* **4065** (2000) 801.
18) C. R. Phipps, J. Luke, and J. Marquis: 36'h AIAA/ASME/SAE/ASEE Joint Propulsion Conference, Huntsville, AL July 18, 2000. AIAA Journal (2001) in press.
19) C. R. Phipps and M. M. Michaelis: Laser and Particle Beams **12** (1994) 23.
20) Stebani, O. Nuyken, T. Lippert, and A. Wokaun: Makromol. Chem. Rapid Commun. **14** (1993) 365.
21) J. Wei, N. Hoogen, T. Lippert, O. Nuyken, and A. Wokaun: J. Phys. Chem. B **105** (2001) 1267.
22) C. David and D. Hambach: Microelect. Engineering **46** (1998) 219.
23) J. E. Andrews, P. E. Dyer, D. Forster, and P. H. Key: Appl. Phys. Lett. **43** (1983) 717.
24) R. Srinivasan and B. Braren: J. Polym. Sci. **22** (1984) 2601.
25) T. Lippert, L. S. Bennett, T. Nakamura, H. Niino. A. Ouchi, and A. Yabe: Appl. Phys. A **63** (1996) 257.
26) T. Lippert, L. S. Bennett, T. Nakamura, H. Niino, A. Ouchi, and A. Yabe: Appl. Surf. Sci. **96-98** (1996) 601.
27) H. Furutani, H. Fukumura. H. Masuhara, T. Lippert, and A. Yabe: J. Phys. Chem. A **101** (1997) 5742.
28) T. Lippert, E. Ortelli, J.-C. Panitz, F. Raimondi, J. Wambach. J. Wei, and A. Wokaun: Appl. Phys. A **69** (1999) S651.
29) C. R. Phipps, T. P. Turner, R. F. Harrison, G. W. York, W. Z. Osborne, G. K. Anderson, X. F. Corlis, L. C. Haynes, H. S. Steele, K. C. Spicochi, and T. R. King: J. Appl. Phys. **64** (1988) 1083.
30) O, Nuyken, J. Stebani, T. Lippert, A. Wokaun, and A. Stasko: Macromol. Chem. Phys. **196** (1995) 751.